RAPID COMMUNICATIONS

PHYSICAL REVIEW B VOLUME 34, NUMBER 9 1 NOVEMBER 1986

Low-temperature phases of Xe on graphite

Timothy Halpin-Healy
Department of Physics, Harvard University, Cambridge, Massachusetts 02138

Mehran Kardar
Department of Physics, Harvard University, Cambridge, Massachusetts 02138
*and Department of Physics, Massachusetts Institute of Technology, Cambridge, Massachusetts 02139**
(Received 9 July 1986)

Light and superlight wall energies for a xenon monolayer on graphite are calculated by a classical, zero-temperature relaxation scheme. Phase diagrams are then obtained using a striped helical Potts model for domain wall networks (such as striped or hexagonal incommensurate solids). The commensurate-incommensurate transition noted in past electron diffraction experiments is reinterpreted as a structural transition between two incommensurate solids, in agreement with recent x-ray scattering work. Matching experimental transition lines lead to estimates for various interatomic potentials. We discuss the preemption of the incipient commensurate phase by condensation of the bilayer.

Despite a large number of experimental studies,[1-3] the low-temperature properties of monolayer xenon adsorbed on graphite are not completely understood. In early transmission high-energy electron diffraction (THEED) experiments, Schabes-Retchkiman and Venables[1] (SRV) reported an hexagonal incommensurate (HIC) to $\sqrt{3}\times\sqrt{3}$ commensurate (C) transition at coverages slightly below a monolayer. Recently, Hong, Birgeneau, and Sutton[2] (HBS) performed precision x-ray scattering work in this regime and concluded that the transition may, in fact, take place between two incommensurate (IC) solids; the low-temperature structure being a striped incommensurate (SIC) phase of superlight domain walls. By explicitly calculating the structure factor of a striped superlight network of domain walls, HBS demonstrated the distinction between C and SIC diffraction signatures—the difference is slight, explaining any possible misidentification in earlier, lower resolution THEED experiments. The possibility that there may be no commensurate phase at all in physisorbed xenon raises some interesting questions, such as the role played by bilayer condensation. In this Rapid Communication we address this issue, as well as other questions relevant to low-temperature phases of Xe on graphite.

In principle, for a simple inert gas such as xenon on graphite, it should be possible to obtain phase diagrams starting from interatomic potentials (a similar program was reasonably successful for Kr on graphite[4]). Unfortunately, the important parameters (V_0, the mean adsorption energy for a single Xe atom on graphite and U_m, the Xe on graphite modulation potential) are not completely known, different choices of V_0 and U_m leading to qualitatively different phase diagrams. For a given modulation potential, we perform a $T=0$ energy relaxation calculation to determine light and superlight wall energies. These energies are then incorporated in a striped helical Potts model of *sparse* domain walls to investigate the low-temperature phases. The somewhat dated Xe-C parameters due to Steele[5] (which imply a weak modulation of $U_m=36$ K) lead to a direct first-order transition from HIC to bilayer structures as the temperature is dropped at fixed pressure. This is in disagreement with the observation of an intermediate phase by SRV and HBS. By choosing a stronger modulation potential, we indeed observe an intermediate striped phase, confirming the interpretation of HBS. Fits to the experimental data of SRV are optimized by the choice of parameters $V_0=2040$ K and $U_m=75$ K. The latter is close to recent first-principles calculations of Vidali and Cole[6] ($U_m=77$ K) or Joos, Bergersen, and Klein[7] ($U_m=75.4$ K). Although the larger modulation potential leads to a SIC phase, it is still not strong enough to stabilize a C phase. The C phase is preempted by a first-order transition between SIC and bilayer solids. Energetic considerations and the precise location of the bilayer condensation line permit us to estimate the second-layer adatom-substrate interaction energy ($\varepsilon_{2s}\sim 150$ K), perhaps the least well-known bilayer parameter.

The specifics of the Xe *adatom* Lennard-Jones (LJ) potential ($\varepsilon=236$ K, $\sigma=3.92$ Å) cause us to decompose the lattice of adsorption sites, which are the centers of the graphite hexagons, into three equivalent triangular sublattices (labeled a, b, and c), of lattice constant $a=4.26$ Å. The well-known $\sqrt{3}\times\sqrt{3}$ commensurate solid, exhibited in Kr and He monolayers, corresponds to perfect occupation of one of these sublattices. At coverages slightly below that associated with a commensurate monolayer ($n=1.0$), vacancies in the Xe on graphite system are accommodated via sparse domain walls which form as neighboring xenon patches switch sublattice occupation. An examination of the microscopic situation reveals that there are, in fact, two types[8] of domain wall: light and superlight, each with its own crossing (Fig. 1). Despite the energy cost associated with domain-wall formation, there is a chemical potential deficit tied to their creation. Hence, for low enough chemical potential, hexagonal and, perhaps, striped arrays of sparse domain walls (IC solids) will be favored over the C structure. Not long ago, the authors[9] introduced the

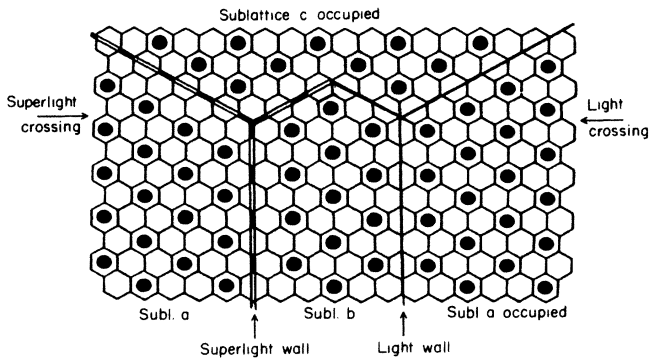

FIG. 1. Domain-wall structures in single-layer Xe on graphite.

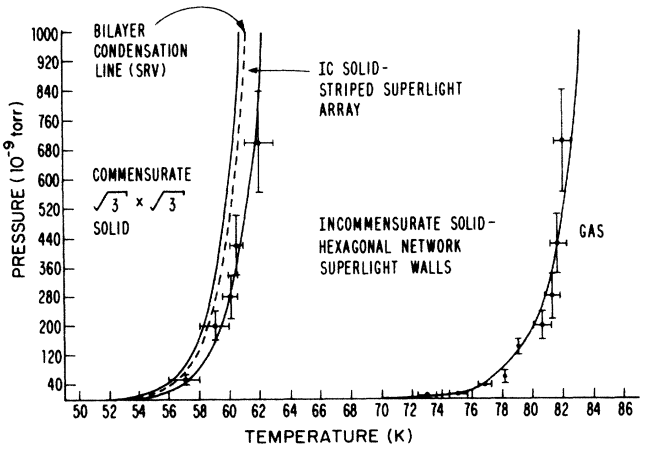

FIG. 2. pT diagram obtained from striped helical Potts model of sparse domain walls in the xenon monolayer. The data points are the result of electron-diffraction studies. Note the SRV bilayer condensation line. Its precise location in our phase diagram suggests that single-layer Xe on graphite is always IC, the C solid preempted by formation of the bilayer. At these low temperatures, bilayer condensation proceeds from a striped IC solid, in agreement with recent x-ray data.

striped helical Potts model, a simple statistical mechanical system that possesses the topological characteristics (three-sublattice degeneracy, wall and crossing helicity, striped and hexagonal phases) exhibited by sparse domain wall networks in Xe monolayers. Indeed, an explicit connection to the energetics of the physisorbed system is even possible[8]—one groups the adsorption sites presented by the basal plane of graphite into large hexagonal patches of size l, the centers of these patches forming the triangular lattice upon which the striped helical Potts model is defined. Sublattice occupation of the Xe adatom patch is dictated by the value (a, b, or c) of the Potts variable governing the patch. Neighboring patches with unequal Potts spins are separated by a wall segment, there being a chemical potential deficit per unit length of $\frac{2}{3}\mu$ for a superlight segment, half that amount for a light segment. Here, μ is the lattice chemical potential. The associated energy costs are denoted J_{SL} and J_L. Crossings of energy X_{SL} and X_L arise when a trio of neighboring patches lack a common Potts spin. In this way, one writes[9] the plaquette energies of the striped helical Potts model in terms of the lattice chemical potential, wall and crossing energies,

$$F = \mathcal{E}(a^{a}_{a}) = \frac{3}{2T} l^2 (\mu + 751 + \frac{2}{3} U_m),$$

$$P = \mathcal{E}(a^{c}_{b}) = \frac{3}{2T} l (-\frac{2}{3}\mu - J_{SL}) - \frac{1}{T} X_{SL} + F,$$

$$N = \mathcal{E}(a^{b}_{c}) = \frac{3}{2T} l (-\frac{1}{3}\mu - J_L) - \frac{1}{T} X_L + F,$$

$$D = \mathcal{E}(a^{c}_{a}) = \frac{\sqrt{3}}{2T} l (-\frac{2}{3}\mu - J_{SL}) + F,$$

$$U = \mathcal{E}(a^{b}_{a}) = \frac{\sqrt{3}}{2T} l (-\frac{1}{3}\mu - J_L) + F.$$

Plaquettes related by a cyclic permutation of spins have the same energy. 751 K results from summing all intralayer two-body Xe-Xe LJ interactions. The LJ parameter of $\varepsilon = 236$ K also includes substrate mediated interactions.[10] Hence, with U_m the Xe on graphite modulation potential, the quantity $(751 + \frac{2}{3}U_m)$ represents the energy per adatom in a perfect, defect-free C phase. The precise value of U_m is not well known and has been the subject of much debate.[6,7] With our own estimate $U_m = 75$ K (this value is justified *a posteriori* by optimizing the fit to experimental data; see Fig. 2), we performed a $T = 0$ energy relaxation calculation to determine the light and superlight wall energies. The resulting wall structures are slightly tighter than those shown in Figs. 8 and 9 of Ref. 2; the corresponding energies, due to off-site relaxation of the adatoms, are $J_{SL} = 95$ K, $J_L = 79$ K. This procedure determines the hard-core width of the walls as well, which fixes the hexagon size to be $l = 4$. Determination of the crossing energies is, in principle, straightforward, but in practice quite a subtle matter.[11] Figure 1 suggests, on physical grounds,[8] that $X_L \approx \frac{3}{2} J_L = 119$ K, since the adatoms have little room to relax. By contrast, X_{SL} involves substantial relaxation, thereby invalidating such naive treatment. Nonetheless, from our past work,[9,12] we know that the maximum temperature of the striped phase will be dictated by the superlight crossing energy. The diffraction profiles of HBS are consistent with a striped phase of superlight walls for a temperature at least as high as ~ 70 K. On the other hand, the wealth of x-ray data in the vicinity of the monolayer triple-point temperature (99 K) make it unlikely that the striped phase extends above 80 K. In this manner, we fix $X_{SL} = 70$ K, which yields $T_{\text{stripe}}^{\text{MAX}} \sim 76$ K. Our independent result lends strong support to the recent estimates of Vidali and Cole[6] ($U_m = 77$ K) and Joos *et al.*[7] ($U_m = 75.4$ K). Conversely, the Steele modulation potential results in wall energies ($J_{SL} < 0$; i.e., energetically *favorable* superlight walls) that necessitate bilayer condensation proceeding from the HIC solid. This precludes the possibility of an intermediate phase and disagrees with all available experimental data.

With the wall and crossing energies fixed, construction of a μT phase diagram is a simple matter. One specifies the chemical potential and temperature—this determines the bare plaquette energies. The phase assumed by the actual Xe monolayer is then ascertained by following the renormalization-group (RG) flows of the striped helical Potts model to the predestined sink. A hexagonal array of superlight walls, for example, is signaled by the growing

dominance, under repeated rescalings, of the P plaquette; similarly, a striped superheavy phase by the D plaquette. One can also determine the monolayer condensation line at the low temperatures of interest by setting $P=0$. This is valid because the gas phase is well represented by a zero (pure vacancy) plaquette,[4] with no energy or chemical potential contributions. A prefacing transformation introduced by Caflisch, Berker, and Kardar,[4] which integrates out the vibrational motions of the registered atoms (thereby relating the Xe adatom chemical potential to the lattice μ of the striped helical Potts model), allows us to write

$$\mu=\mu_{\text{adatom}}+T\sum\ln[\tfrac{1}{2}\operatorname{csch}(\omega_a/T)]+V_0\ .$$

Here, $V_0=2040$ K is the mean adatom-surface energy which optimizes our fit to the electron diffraction data and $\omega_x=\omega_y=43$ K, $\omega_z=49$ K are the characteristic frequencies ($h=k=1$) which follow from a harmonic approximation applied to the assumed LJ potentials. [Although our value for V_0 is somewhat higher than the Vidali-Cole[6] estimate (1910 K), it is quite close to other empirical values calculated by Joos *et al.*[7] (2005 K) and Klein, O'Shea, and Ozaki[13] (2020 K). An analysis[14] of adsorption isotherm data in the Henry's law region has yielded 1928 K, but more recent experimental work[15] suggests that $V_0\gtrsim 2000$.] For a xenon monolayer in equilibrium with ambient ideal gas vapor, $\mu_{\text{adatom}}=\mu_{\text{gas}}=T\ln(p\lambda^3/T)$, with thermal wavelength $\lambda=1\sqrt{2\pi mT}$. Thus, we transcribe the phase boundaries in μT space to obtain the experimentally relevant pT diagram shown in Fig. 2. It is apparent that the transition lines agree very well with the experimental data points,[2,16] while simultaneously confirming the HBS interpretation of the monolayer structural transition. We stress that these lines are essentially zero-temperature results, the separation of the D-P and P-gas lines determined by J_{SL} (and, to a much lesser degree, X_{SL}), while V_0 pins down their exact location. The agreement with experiment therefore reflects the correct determination of the *energies* of the model from the relaxation method. *Entropy* effects, included via the RG, play a minor role at these temperatures. (They lead, for example, to a dislocation-dominated fluid phase between the HIC and SIC phases which covers too small a region to be visible in Fig. 2.)

Furthermore, SRV report in their isobaric scans, formation of a second layer (dashed line), just 0.7–1.0 K after the purported HIC-C transition. It is evident that the C phase of our model (which so far includes no second-layer physics) is preempted by bilayer condensation, which proceeds by a strong first-order transition from a striped phase of superlight domain walls, as pointed out by HBS. We mention our own attempt to reproduce this experimental line via simple energetic considerations. Good agreement necessitates a second-layer adatom-substrate energy $\varepsilon_{2s}\sim 150$ K, somewhat less than the value (~ 300 K) expected from a naive 3–12 LJ potential with $V_0=2040$ K, $z_{\min}=3.34$ Å. (The total energy is obtained by adding the attraction to the first layer.[4]) There appears to be substantial screening of the xenon-substrate and substrate mediated interactions (see below) by the first xenon layer. It would be interesting to directly confirm this observation either theoretically by a first-principles calculation including many-body effects, or experimentally by the scattering of xenon from Xe-preplated graphite.

In Fig. 3 we sketch the coverage versus temperature (nT) phase diagrams implicitly suggested by the two experimental groups.[17] Figure 3(a) shows the nT diagram consistent with the recent x-ray scattering work of HBS. Note that the IC striped monolayer solid (topped by second-layer gas) coexists with a bilayer structure below temperatures ~ 76 K, with the bilayer low-density coexistence boundary intercepting the coverage axis at $n=1.0$. The SIC solid, a $T=0$ phase existing over a range of coverages,[12] eventually gives way to the HIC structure at lower n. More low-T, precision x-ray work is needed to determine exactly the locations of the intercepts. Another interesting aspect of this phase diagram is the temperature-driven structural transition between IC striped and hexagonal solids. This is most likely due to the entropic effect of breathing modes in the HIC phase,[18] a feature not present in our model. Lastly, note that the second-layer critical temperature T_{c2} exceeds that of the monolayer, an illus-

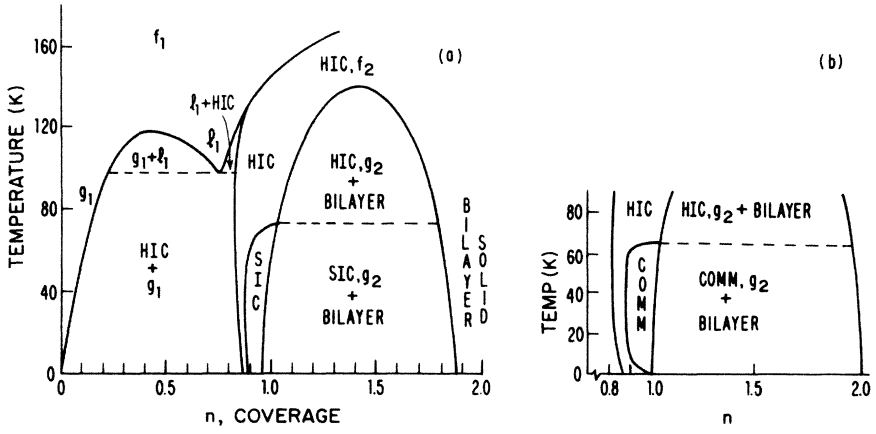

FIG. 3. (a) Full nT diagram, through bilayer coverage, in accord with HBS. g_1, l_1, and f_1 denote gas, liquid, and fluid phases in the first layer, similarly for g_2,f_2. Note the low-temperature phase boundaries near monolayer coverage. (b) That portion of the previous diagram which is altered by the interpretation of SRV in terms of a C-IC transition.

trative manifestation of the reduction of substrate-mediated interactions mentioned earlier. As Monte Carlo simulation[19] and virial calculations[20] predict $T_{c2} \approx 0.50\varepsilon_{LJ}^{Xe}$, the precise experimental determination of T_{c2} would provide a measure of the LJ interactions of the second-layer xenon atoms. Because x-ray work[3] indicates that bilayer Xe already closely resembles the bulk $3d$ crystal, we expect $T_{c2} \sim 130$–140 K, as $\varepsilon_{LJ}^{3dXe} = 281$ K.

By comparison, the simplest nT diagram consistent with the SRV interpretation of their own THEED data is shown in Fig. 3(b). In this case, the low-temperature coexistence involves commensurate and bilayer solids. Nonetheless, because the zero-temperature commensurate solid can exist only at $n = 1.0$ (defects cannot be accommodated), the C phase must pinch off at $T = 0$. This necessitates a second, lower-temperature HIC-C transition in which the C solid is thermally stabilized, an extremely unlikely scenario, given the naturally expanded state of the xenon monolayer.[21] (Recall that the Xe LJ minimum occurs at $r = 4.41$ Å, while the commensurate spacing is 4.26 Å.)

With light and superlight wall energies determined by a classical, zero-temperature energy relaxation scheme, we have investigated the properties of sparse domain wall networks in the xenon monolayer. A prefacing transformation permitted construction of a pT diagram with transition lines in fine agreement with existing electron diffraction data, as well as the HBS interpretation of the monolayer structural transition. Optimizing the fit to experiment, we find $U_m = 75$ K and $V_0 = 2040$ K. Our results also suggest that the Xe monolayer is *always* incommensurate—formation of the bilayer preempting any possible commensurate phase. It is our hope that future x-ray experiments will concentrate on the interesting physics exhibited by low-temperature near-monolayer Xe on graphite.

We have benefited from discussions with R. J. Birgeneau and H. Hong. One of us (M.K.) was partly supported by the Society of Fellows at Harvard University and by the U. S. Army Research Office under Contract No. DAAG 29-85-K-0058 at Massachusetts Institute of Technology. This research was supported by the National Science Foundation through Grant No. DMR 85-14638.

---

*Present address.

[1]P. S. Schabes-Retchkiman and J. A. Venables, Surf. Sci. **105**, 536 (1981).

[2]H. Hong, R. J. Birgeneau, and M. Sutton, Phys. Rev. B **33**, 3344 (1986).

[3]See P. A. Heiney, P. W. Stephens, R. J. Birgeneau, P. M. Horn, and D. E. Moncton, Phys. Rev. B **28**, 6416 (1983), for discussion and an exhaustive list of references.

[4]R. G. Caflisch, A. N. Berker, and M. Kardar, Phys. Rev. B **31**, 4527 (1985).

[5]W. A. Steele, Surf. Sci. **36**, 317 (1973).

[6]G. Vidali and M. W. Cole, Phys. Rev. B **29**, 6736 (1984).

[7]B. Joos, B. Bergersen, and M. L. Klein, Phys. Rev. B **38**, 7219 (1983).

[8]M. Kardar and A. N. Berker, Phys. Rev. Lett. **48**, 1552 (1982).

[9]T. Halpin-Healy and M. Kardar, Phys. Rev. B **31**, 1664 (1985).

[10]S. Rauber, J. R. Klein, and M. W. Cole, Phys. Rev. B **27**, 1314 (1983).

[11]Refer to M. Schobinger and F. F. Abraham, Phys. Rev. B **31**, 4590 (1985); A. L. Talapov, *ibid.* **24**, 6703 (1981), for an indication of the difficulties associated with calculating the crossing energy in an adsorbed monolayer system, in this case Kr on graphite.

[12]T. Halpin-Healy and M. Kardar, Phys. Rev. B (to be published).

[13]M. L. Klein, S. O'Shea, and Y. Ozaki, J. Phys. Chem. **88**, 1420 (1984).

[14]T. R. Rybolt and R. A. Pierotti, J. Phys. Chem. **70**, 4413 (1979).

[15]J. Piper and J. A. Morrison, Chem. Phys. Lett. **103**, 323 (1984).

[16]The low pressure points on the monolayer condensation line are from J. Suzanne, J. P. Coulomb, and M. Bienfait, Surf. Sci. **47**, 204 (1976).

[17]We have not included an unsuccessful phase diagram resulting from our own RG studies of a related, but distinct xenon Potts *lattice-gas* model, which overestimates the maximum temperature of the solid phases. This difficulty is probably associated with the breakdown, at high temperatures, of the basic picture of commensurate domains separated by walls.

[18]J. Villain, in *Ordering in Strongly Fluctuating Condensed Matter Systems,* edited by T. Riste (Plenum, New York, 1980), p. 221.

[19]F. F. Abraham, Phys. Rep. **80**, 339 (1981).

[20]J. R. Klein and M. W. Cole, Faraday Discuss. Chem. Soc. **80**, 1 (1985).

[21]A thermally stabilized commensurate phase is conceivable in krypton physisorbed on graphite, though, because of the natural contractive tendency of Kr (LJ minimum at $r = 4.05$ Å). See S. W. Koch and F. F. Abraham, Phys. Rev. B **33**, 5884 (1986).